

## Phase Field Model of Thermo-Induced Marangoni Effects in the Mixtures and its Numerical Simulations with Mixed Finite Element Method

Pengtao Sun<sup>1,\*</sup>, Chun Liu<sup>2</sup> and Jinchao Xu<sup>2</sup>

<sup>1</sup> *Department of Mathematical Sciences, University of Nevada, Las Vegas, 4505 Maryland Parkway, Las Vegas, NV 89154, USA.*

<sup>2</sup> *Department of Mathematics, The Pennsylvania State University, University Park, PA 16802, USA.*

Received 29 October 2008; Accepted (in revised version) 30 March 2009

Communicated by Pingwen Zhang

Available online 14 May 2009

---

**Abstract.** In this paper, we study the Marangoni effects in the mixture of two Newtonian fluids due to the thermo-induced surface tension heterogeneity on the interface. We employ an energetic variational phase field model to describe its physical phenomena, and obtain the corresponding governing equations defined by a modified Navier-Stokes equations coupled with phase field and energy transport. A mixed Taylor-Hood finite element discretization together with full Newton's method are applied to this strongly nonlinear phase field model on a specific domain. Under different boundary conditions of temperature, the resulting numerical solutions illustrate that the thermal energy plays a fundamental role in the interfacial dynamics of two-phase flows. In particular, it gives rise to a dynamic interfacial tension that depends on the direction of temperature gradient, determining the movement of the interface along a sine/cosine-like curve.

**AMS subject classifications:** 65B99, 65K05, 65K10, 65N12, 65N22, 65N30, 65N55, 65Z05

**Key words:** Phase field, Navier-Stokes equations, Marangoni effects, temperature dependent surface tension, mixed Taylor-Hood finite element, Newton's method.

---

## 1 Introduction

Phase field models are an increasingly popular choice for modeling the motion of multi-phase fluids (see [3] for a recent review). In the phase-field model, sharp fluid interfaces

---

\*Corresponding author. *Email addresses:* pengtao.sun@unlv.edu (P. Sun), liu@math.psu.edu (C. Liu), xu@math.psu.edu (J. Xu)

are replaced by thin but nonzero thickness transition regions where the interfacial forces are smoothly distributed [9]. The basic idea is to introduce a conserved order parameter (e.g., mass concentration) that varies continuously over thin interfacial layers and is mostly uniform in the bulk phases. These models allow topological changes of the interface [6, 18, 19, 25] and have many advantages in numerical simulations of the interfacial motion [12]. Thus, it is also known as the diffuse-interface model. More precisely, in this work, a phase-field variable  $\phi$  is introduced, which can be thought of as the volume fraction, to demarcate the two species and indicate the location of the interface. A mixing energy is defined based on  $\phi$  which, through a convection-diffusion equation, governs the evolution of the interfacial profile. The phase-field method can be viewed as a physically motivated level-set method, and Lowengrub and Truskinovsky [25] have argued for the advantage of using a physically determined  $\phi$  profile instead of an artificial smoothing function for the interface. When the thickness of the interface approaches zero, the diffuse-interface model becomes asymptotically identical to a sharp-interface level-set formulation. It also reduces properly to the classical sharp-interface model in general. Recently many researchers have employed the phase field approach for various fluid models [2, 4–6, 13–15, 18–20, 24, 26, 29, 33]. Based on an energetic variational formulation, Liu and Shen [22] employed a phase field model to describe the mixture of two incompressible Newtonian fluids. The mixing energy studied is related to the usual Ginzburg-Landau model for phase evolutions.

The study of the evolution of the free interfaces is one of the most important fundamental area in the theory of hydrodynamics and rheology. The analytical and numerical analysis of these problems has attracted attention for more than one hundred years, where the Marangoni effect is a typical model. Marangoni effects [35, 36] are due to the inhomogeneity of the interfacial properties. The effects can be attributed to either the non-uniform distributions of particles (surfactants) or the distribution of temperatures which is the case we will study in this paper. This ubiquitous phenomena (such as wine tears) had been studied for more than 150 years since James Thomson, Carlo Marangoni and Willard Gibbs. It is involved in almost all studies of free interface and interface properties. The Marangoni-Benard convection is one of the most fascinating phenomenon in fluids. It has becoming more and more important in the application of non-Newtonian fluids and ocean-geophysical dynamics.

The conventional Marangoni-Benard convection is described by the following two phase fluids with a sharp interface, involving the Boussinesq approximation

$$\rho(u_t + (u \cdot \nabla)u) + \nabla p - \nu \operatorname{div} D(u) = -\rho_\theta g j, \quad (1.1)$$

$$\nabla \cdot u = 0, \quad (1.2)$$

$$\theta_t + u \cdot \nabla \theta = k \Delta \theta, \quad (1.3)$$

where  $u$ ,  $p$  and  $\theta$  stand for the fluid velocity, pressure, and temperature, respectively.  $\rho$  is the density of fluid mixture,  $\rho_\theta$  is the temperature-dependent density defined as

$$\rho_\theta = \rho[1 - \alpha(\theta - \theta_0)], \quad (1.4)$$

$\theta_0$  is the ambient temperature,  $\alpha$  is the coefficient of thermal expansion,  $g$  is the gravitational acceleration,  $j$  is the upward direction, and  $k$  is the thermal diffusion. With the usual initial and boundary conditions, the interface conditions take the form

$$\varepsilon_t + u \cdot \nabla \varepsilon = 0, \quad (1.5)$$

$$[T] \cdot n = -\sigma H n + (t \cdot \nabla \sigma) t, \quad (1.6)$$

where  $\varepsilon$  indicates the interface length of the mixture. Eq. (1.5) is the kinematic condition, representing the surface ( $\varepsilon=0$ ) evolve with the fluid.  $H$  is the curvature of the interface, and (1.6) is the traction free boundary (balance of forces on the interface) condition, where  $T = -pI + \nu D(u)$  is the jump of the stress across the interface  $\Gamma_t$ ,  $n$  its normal and  $t$  its tangent. The surface tension  $\sigma$  linearly depends on the temperature, shown as  $\sigma = a - b\theta$ .

The statistical (or phase field approach) point of view represents the interface as a continuous, but steep, change of properties (density, viscosity etc) of the two fluids. Within a "thin" transition region, the fluid is mixed and has to store certain amount of "mixing energy". Such an approach coincides with the usual phase field models in the theory of phase transition (see, e.g., [10, 11, 27, 28, 31] and many others).

To study the free interface between two Newtonian fluids with different densities and viscosities, Shkoller and Liu [23] proved that the variational phase field models will converge to the original Navier-Stokes equation with both the kinematic and kinetic boundary condition on the interface. The convergence is understood in the usual viscosity solution sense [17]. In our earlier works [22–24], we have utilized an energetic variational approach with a phase field formulation. It is the coupling between the elastic stress (due to the mixing) and the transport of the fluid indicator function (the phase) that represents the interaction between the interfaces and the flow fields. At the same time, such a special coupling also preserves the dissipative nature of the system.

Numerical simulations also demonstrate that the method captures many interesting physical phenomena and at the same time is very robust [22]. The key observation is that in the phase field model, the surface force (such as surface tension) can be viewed as the limit of the bulk body force as the thickness of the interface approaches zero [24].

In this paper, we are interested in the phase field model arising from thermo-induced Marangoni effects in the mixtures, modeled as (2.1) containing a modified Navier-Stokes equation, phase field and energy transport equations. We will show that this model converges to the original system (1.1)-(1.3). Moreover, it represents a mechanism for certain degree of transition (mixing) in terms of thermo-induced surface tension. In the numerical implementation, we employ a type of mixed Taylor-Hood finite element method combining with Newton's method to discretize this model. The resulting numerical solutions reveal the dramatic phenomena of thermo-induced surface tension transformation, which basically match with the real physical cases as well.

Here follows the general layout of the paper: in Section 2, we describe the phase field system on thermo-induced Marangoni effects in the mixtures, present a phase field model combining with energy transport and a modified Navier-Stokes equations containing temperature-dependent surface tension. Our numerical method are presented in

Section 3, a mixed Taylor-Hood finite element discretization and full Newton's method are applied to this strongly nonlinear phase field model. Based on these algorithms, in Section 4 we carry out the numerical experiments on a couple of typical physical cases, the corresponding elucidations of numerical solutions are also given.

## 2 A phase field model for thermo-induced Marangoni effects in the mixtures

Without loss of generality, let us start with the case with linear coefficients. A phase field model describing thermo-induced Marangoni effects in the mixtures can be given as follows

$$u_t + (u \cdot \nabla)u + \nabla p - \nu \operatorname{div} D(u) + \nabla \cdot \left( \lambda \nabla \phi \otimes \nabla \phi - \frac{\lambda}{2} |\nabla \phi|^2 - \frac{\lambda}{2\epsilon^2} (\phi^2 - 1)^2 \right) = -\rho_\theta g j, \quad (2.1)$$

$$\nabla \cdot u = 0, \quad (2.2)$$

$$\phi_t + u \cdot \nabla \phi + \gamma \Delta (\Delta \phi - f(\phi)) = 0, \quad (2.3)$$

$$\theta_t + u \cdot \nabla \theta = k \Delta \theta, \quad (2.4)$$

with initial conditions

$$u|_{t=0} = u_0, \quad \phi|_{t=0} = \phi_0, \quad \theta|_{t=0} = \theta_0, \quad (2.5)$$

and appropriate boundary conditions, where  $x \in \Omega \subset R^d$ ,  $t \in [0, T]$ ,  $T > 0$  is the maximum evolution time,  $\Omega$  is a bounded, connected Lipschitz domain in  $R^d$ ,  $d$  is spatial dimension. As usual, we assume that  $\Omega$  is a polygon. Here we consider the mixture of two Newtonian flow under gravity force and adopt the Boussinesq approximation in the system. In (2.1),  $D(u) = (1/2)(\nabla u + (\nabla u)^T)$  is the stretching tensor,  $\lambda = \epsilon \sigma = \epsilon(a - b\theta)$  is the surface tension parameter. In (2.3),  $\gamma$  represents the elastic relaxation time. As  $\gamma \rightarrow 0$ , the limiting  $\phi$  satisfies the transport equation, which is equivalent to the mass transport equation (for incompressible fluids). Hence this formulation can also be viewed as the link (relaxation) between the mass average (in the kinetic energy) and the volume average (in the elastic energy) between the two species.

The "phase" function  $\phi(x, t)$  is employed to identify the regions that two fluid flows occur:  $\{x: \phi(x, t) = 1\}$  is occupied by fluid phase I and  $\{x: \phi(x, t) = -1\}$  by fluid phase II. Following the work in [22], we suppose that the elastic (mixing) energy is in the following form

$$W(\nabla \phi, \phi) = \int_{\Omega} \frac{1}{2} |\nabla \phi|^2 + F(\phi) dx. \quad (2.6)$$

We can view  $\phi$  as volume fraction. The mixing density and viscosity will be functions of  $\phi$ . In (2.3),  $f(d)$  is a polynomial of  $d$  such that  $f(\phi) = F'(\phi)$ , where

$$F(\phi) = \frac{(\phi^2 - 1)^2}{4\epsilon^2}$$

is the bulk part of the mixing energy, so

$$f(\phi) = \frac{1}{\varepsilon^2}(\phi^2 - 1)\phi.$$

The part of bulk energy represents the interaction of different volume fractions of individual species (like Flory-Huggins free energy [16,21]). The gradient part plays the role of regularization (relaxation). The interface is represented by  $\{x : \phi(x,t) = 0\}$ , with the fixed transition layer of thickness  $\varepsilon$ .

The dynamics of the phase field  $\phi$  can be driven by either Allen-Cahn or Cahn-Hilliard types of gradient flow [1], depending on the choice of dissipative mechanism. The former leads to the Allen-Cahn equation

$$\phi_t + u \cdot \nabla \phi = -\gamma \frac{\delta W}{\delta \phi} = \gamma(\Delta \phi - f(\phi)), \tag{2.7}$$

while the latter leads to the Cahn-Hilliard equation:

$$\phi_t + u \cdot \nabla \phi = \nabla \cdot \left( \gamma \nabla \frac{\delta W}{\delta \phi} \right) = -\gamma \Delta(\Delta \phi - f(\phi)), \tag{2.8}$$

where  $\frac{\delta W}{\delta \phi}$  represents the variation of the energy  $W$  with respect to  $\phi$ .

It is obvious that the solutions of (2.8) satisfy the following energy law

$$\frac{d}{dt} \int_{\Omega} \frac{1}{2} |\nabla \phi|^2 + F(\phi) dx = - \int_{\Omega} \gamma \left| \nabla \frac{\delta W}{\delta \phi} \right|^2 dx = - \int_{\Omega} \gamma |\nabla(\Delta \phi - f(\phi))|^2 dx. \tag{2.9}$$

This energy dissipative relation shows the variation natural of the Cahn-Hilliard equation.

We now describe the governing equations for the fluid flow. When the surface tension is a constant, the system of the Cahn-Hilliard equation coupled with the momentum equation (1.1) give the following energy estimate [22]

$$\frac{d}{dt} \int_{\Omega} \frac{1}{2} |u|^2 + \frac{\lambda}{2} \left( |\nabla \phi|^2 + F(\phi) \right) dx = - \int_{\Omega} \nu |\nabla u|^2 + \gamma \lambda |\nabla(\Delta \phi - f(\phi))|^2 dx. \tag{2.10}$$

From the derivation of the energy law, we notice the cancelation of the induced stress term in the momentum equation and the special transport property of the phase variable  $\phi$ .

In case of  $\lambda$  as a function of both time and the space, we can still consider the following action function

$$A(x) = \int_0^T \int_{\Omega_0} \frac{1}{2} |x_t(X,t)|^2 + \frac{\lambda(x(X,t),t)}{2} \left( |\nabla_x \phi(x(X,t),t)|^2 + F(\phi(x(X,t),t)) \right) dX dt. \tag{2.11}$$

Here we can view  $X$  as the Lagrangian (initial) material coordinate and  $x(X,t)$  the Eulerian (reference) coordinate.  $\Omega_0$  is the initial domain occupied by the fluid. The notion that  $\phi(x(X,t),t)$  indicated that  $\phi$  is transported by the flow field (moving along trajectory).

For incompressible materials, we look at the volume preserving flow maps  $x(X,t)$  such that

$$x_t(X,t) = v(x(X,t),t), \quad x(X,0) = X. \tag{2.12}$$

The least action principle will yield the linear momentum equation (force balance), without the viscosity terms. Suppose we have a one parameter family of such maps  $x^\varepsilon$  such that

$$x^0 = x, \quad \frac{dx^\varepsilon}{d\varepsilon} = y, \tag{2.13}$$

for any  $y$  such that  $\nabla_x \cdot y = 0$ . We compute the variation of  $A(x^\varepsilon) = A(\phi(x^\varepsilon, t))$  with respect to  $\varepsilon$  and evaluated at  $\varepsilon = 0$  and obtain

$$u_t + (u \cdot \nabla)u - \nabla \cdot (v \nabla u) + \nabla p + \nabla \cdot \left( \lambda \nabla \phi \otimes \nabla \phi - \frac{\lambda}{2} |\nabla \phi|^2 - \frac{\lambda}{2\varepsilon^2} (\phi^2 - 1)^2 \right) = 0. \tag{2.14}$$

Here we also absorb all the pure gradient terms into the pressure.

The constant  $\varepsilon$  represents the capillary length of the mixture [7, 8, 30]. As the constant  $\varepsilon$  approaches zero,  $\phi$  will approach to 1 and  $-1$  almost everywhere and the induced stress will give a measure valued force that supported only on the interface between  $\{\phi = 1\}$  and  $\{\phi = -1\}$ . Moreover  $W(\phi)$  is uniformly bounded in time  $t$ .

We can formally compute the limit of the induced force term and get that [22]

$$\lambda \nabla \cdot (\nabla \phi \otimes \nabla \phi) = \lambda a^2 Hn + \lambda \nabla \frac{1}{4\varepsilon^2} (\phi^2 - 1)^2 + \lambda \nabla \frac{a^2}{2}. \tag{2.15}$$

Since the interface length  $\varepsilon$  is usually small, so will  $\lambda$  be. However, for each fixed  $\varepsilon$  (hence  $\lambda$ ), the capillary term stabilized the system (in fact, it stabilized the transport of the phase function).

A further computation shows that

$$\begin{aligned} & \nabla \cdot \left( \lambda \nabla \phi \otimes \nabla \phi - \frac{\lambda}{2} |\nabla \phi|^2 - \frac{\lambda}{2\varepsilon^2} (\phi^2 - 1)^2 \right) \\ &= -\lambda \Delta \phi \nabla \phi - \frac{\lambda}{2} \nabla |\nabla \phi|^2 - (\nabla \lambda \cdot \nabla \phi) \nabla \phi \\ & \quad + \frac{\nabla \lambda}{2} |\nabla \phi|^2 + \frac{1}{2\varepsilon^2} \nabla \lambda (\phi^2 - 1)^2 + \frac{1}{2\varepsilon^2} \lambda \nabla (\phi^2 - 1)^2. \end{aligned} \tag{2.16}$$

It can be verified that the right hand side converges to

$$-\sigma Hn + \nabla \sigma - (\nabla \sigma \cdot n)n = -\sigma Hn + (\nabla \sigma \cdot t)t,$$

where  $t$  is the tangential direction of the interface. This recovers the traction free boundary condition (1.6).

If we consider the density  $\rho$ , viscosity  $\nu$  and heat conductivity  $k$  are nonlinear functions associated with the phase  $\phi$ , and the coefficients of temperature-dependent surface tension  $\lambda$  and  $\eta$  are the functions of temperature  $\theta$ , then a more general case of (2.1)-(2.4) can be given as follows

$$(\rho(\phi)u)_t + (u \cdot \nabla)(\rho(\phi)u) + \nabla p - \nabla \cdot (\nu(\phi)\nabla u) + \nabla \cdot \left( \lambda(\theta)\nabla\phi \otimes \nabla\phi - \frac{\lambda(\theta)}{2}|\nabla\phi|^2 - \frac{\lambda(\theta)}{2\varepsilon^2}(\phi^2 - 1)^2 \right) = \rho(\phi)\eta(\theta)gj, \tag{2.17a}$$

$$\nabla \cdot u = 0, \tag{2.17b}$$

$$\phi_t + u \cdot \nabla\phi = \gamma(\Delta\phi - \frac{1}{\varepsilon^2}(\phi^2 - 1)\phi), \tag{2.17c}$$

$$\theta_t + u \cdot \nabla\theta = \nabla \cdot (k(\phi)\nabla\theta), \tag{2.17d}$$

where, instead of Cahn-Hilliard equation (2.3) or (2.8), in this paper we employ Allen-Cahn equation (2.7) to describe phase field equation (2.17c) since its numerical treatment is simpler than that of the Cahn-Hilliard type which involves fourth-order differential operators.

By introducing  $\rho_i, \nu_i, k_i$  ( $i=1,2$ ) as densities, viscosities, and heat conductivities of two Newtonian fluids, we define the following physical coefficient functions of the mixtures: density function

$$\rho(\phi) = \frac{1-\phi}{2}\rho_1 + \frac{1+\phi}{2}\rho_2,$$

viscosity function

$$\nu(\phi) = \frac{1-\phi}{2}\nu_1 + \frac{1+\phi}{2}\nu_2,$$

and heat conductivity function

$$k(\phi) = \frac{1-\phi}{2}k_1 + \frac{1+\phi}{2}k_2.$$

Surface tension coefficient function  $\lambda(\theta)$  is defined as  $\lambda(\theta) = \lambda_0\sigma = \lambda_0(a - b\theta)$ , and  $\lambda_0 = m\varepsilon = ch$  where the interface length  $\varepsilon$  is proportional to mesh size  $h$ . On the right hand side of (2.17a),  $\eta(\theta) = \alpha(\theta - \theta_0) - 1$  via (1.4). The resulting specific parameters  $a, b, \alpha$  and  $\gamma$  in (2.17) are associated with certain physical significance, and should be carefully provided in the numerical experiments later.

The coupled nonlinear system (2.17) is subject to appropriate boundary conditions (2.18) and initial conditions (2.5), where  $\phi_0(x)$  is prescribed on the basis of concrete problems, see the examples shown in Section 4 for more details. The boundary conditions on  $\partial\Omega$  belong to either Dirichlet type or homogeneous Neumann type:

$$u = u_b(x,t), \quad a\frac{\partial\phi}{\partial n} + b\phi = \phi_b(x,t), \quad \theta = \theta_b(x,t), \tag{2.18}$$

where  $u_b, \phi_b$  and  $\theta_b$  represent the boundary value functions of  $u, \phi$  and  $\theta$ , respectively.  $p$  holds free boundary condition on  $\partial\Omega$ . Here the parameters  $a$  or  $b$  may equal zero, depending on whether Dirichlet or Neumann boundary condition is chosen for  $\phi$ .

We assume that the coefficient functions mentioned in (2.17) are all sufficiently smooth, continuous or conceive in order to guarantee the well-posedness of its weak forms and the optimal error estimate in  $H^1$  or  $L^2$  norm holding for its numerical discretizations.

Actually (2.17) involves the Boussinesq approximation with a sharp interface between two phase flows. According to aforementioned phase field theory, we only need to figure out where the solution of phase  $\phi$  equals or closes to zero in order to find the location of this sharp interface. By using phase field method, the interface between fluid mixtures can be obtained more exactly and efficiently in comparison with common tracking methods.

### 3 Numerical methods

In this section we use Newton's method to linearize (2.17) and mixed finite element method to discretize the weak form of corresponding linearization.

#### 3.1 Newton's method

(2.17) is a strongly nonlinear coupling system containing Navier-Stokes, phase field and energy transport equations. In this section we employ Newton's method to linearize (2.17). To this end, first of all, let's introduce a generalized Newton's linearization for a nonlinear equation associated with multiple unknowns  $u, \phi$  and  $\theta$

$$F(u, \phi, \theta) = 0. \quad (3.1)$$

Then Newton's method is processed generally as follows. In the process of nonlinear iteration, suppose the solutions  $(u^n, \phi^n, \theta^n)$  have been obtained at the  $n$ th step, where, if  $n = 0$ , then we directly take the initial guesses of nonlinear iteration  $u^0, \phi^0, \theta^0$ . By letting  $\delta u^{n+1}, \delta \phi^{n+1}, \delta \theta^{n+1}$  be the increments of  $u, \phi, \theta$  at the  $(n+1)$ th step, respectively, we require the new solutions  $(u^{n+1}, \phi^{n+1}, \theta^{n+1})$  at the  $(n+1)$ th step to satisfy the original equation (3.1), where

$$u^{n+1} = u^n + \delta u^{n+1}, \quad \phi^{n+1} = \phi^n + \delta \phi^{n+1}, \quad \theta^{n+1} = \theta^n + \delta \theta^{n+1}. \quad (3.2)$$

Thus we have the following equation in terms of Newton's method

$$\begin{aligned} F(u^{n+1}, \phi^{n+1}, \theta^{n+1}) &= F(u^n + \delta u^{n+1}, \phi^n + \delta \phi^{n+1}, \theta^n + \delta \theta^{n+1}) \\ &\approx F(u^n) + F'_u(u^n, \phi^n, \theta^n) \delta u^{n+1} + F(\phi^n) + F'_\phi(u^n, \phi^n, \theta^n) \delta \phi^{n+1} \\ &\quad + F(\theta^n) + F'_\theta(u^n, \phi^n, \theta^n) \delta \theta^{n+1} = 0, \end{aligned} \quad (3.3)$$

where  $F'_u, F'_\phi, F'_\theta$  are Fréchet derivatives of nonlinear function  $F(u, \phi, \theta)$  with respect to  $u, \phi$  and  $\theta$ , respectively.

Thus, we get Newton's incremental linearization scheme with respect to the unknown increments  $\delta u, \delta \phi, \delta \theta$

$$\begin{aligned} & F'_u(u^n, \phi^n, \theta^n) \delta u^{n+1} + F'_\phi(u^n, \phi^n, \theta^n) \delta \phi^{n+1} + F'_\theta(u^n, \phi^n, \theta^n) \delta \theta^{n+1} \\ &= -F(u^n) - F(\phi^n) - F(\theta^n). \end{aligned} \tag{3.4}$$

By combining with (3.2), we obtain the solutions  $(u^{n+1}, \phi^{n+1}, \theta^{n+1})$  at the  $(n+1)$ th iteration step.

On the other hand, we can also directly find the solutions  $(u^{n+1}, \phi^{n+1}, \theta^{n+1})$  by plugging  $\delta u^{n+1} = u^{n+1} - u^n, \delta \phi^{n+1} = \phi^{n+1} - \phi^n, \delta \theta^{n+1} = \theta^{n+1} - \theta^n$  into (3.4), which leads to Newton's total linearization scheme with respect to unknowns  $u^{n+1}, \phi^{n+1}, \theta^{n+1}$  at the  $(n+1)$ th iteration step

$$\begin{aligned} & F'_u(u^n, \phi^n, \theta^n) u^{n+1} + F'_\phi(u^n, \phi^n, \theta^n) \phi^{n+1} + F'_\theta(u^n, \phi^n, \theta^n) \theta^{n+1} \\ &= F'_u(u^n, \phi^n, \theta^n) u^n + F'_\phi(u^n, \phi^n, \theta^n) \phi^n + F'_\theta(u^n, \phi^n, \theta^n) \theta^n - F(u^n) - F(\phi^n) - F(\theta^n). \end{aligned} \tag{3.5}$$

In accordance with the local quadratic convergence theory of Newton's method, (3.4) or (3.5) should converge provably in very few iteration steps with the proper initial guesses  $u^0, \phi^0$  and  $\theta^0$ . If the equation (3.1) is provided as a time-dependent nonlinear partial differential equation, the initial guesses of nonlinear iteration at the  $k$ th time step are usually given as the solutions of linearized PDE at the previous  $(k-1)$ th time step. If  $k=1$ , then the initial conditions of original time-dependent PDE are taken as the initial guesses of nonlinear iteration at the 1st time step.

In the following we linearize the system of nonlinear PDEs (2.17) by applying Newton's total linearization scheme (3.5) to each nonlinear equation. Provided the solutions  $(u^n, \phi^n, \theta^n)$  are obtained at the  $n$ th iteration step, and let  $(u^{n+1}, \phi^{n+1}, \theta^{n+1})$  be the desired solutions at the  $(n+1)$ th iteration step, we demonstrate a full Newton's linearization for (2.17) as follows.

Applying (3.5) to (2.17a) with respect to unknowns  $u, \phi, \theta$ , respectively, and considering (2.16), we have the following Newton's linearized equation for (2.17a)

$$\begin{aligned} & \rho(\phi^n) u_t^{n+1} + \frac{\rho_2 - \rho_1}{2} \phi_t^n u^{n+1} + T_1^n + T_2^n - \nabla \cdot (\nu(\phi^n) \nabla u^{n+1}) + \nabla p^{n+1} + T_3^n \\ & - \rho(\phi^n) \varphi \alpha g \theta^{n+1} j + \frac{\rho_2 - \rho_1}{2} (u_t^n \phi^{n+1} + u^n \phi_t^{n+1}) + T_4^n - \nabla \cdot \left( \frac{\nu_2^n - \nu_1^n}{2} \phi^{n+1} \nabla u^n \right) + T_5^n \\ &= \frac{\rho_2 - \rho_1}{2} (u_t^n \phi^n + u^n \phi_t^n) - \nabla \cdot \left( \frac{\nu_2^n - \nu_1^n}{2} \phi^n \nabla u^n \right) + S_1^n + S_2^n + S_3^n + S_4^n, \end{aligned} \tag{3.6}$$

where

$$\begin{aligned} T_1^n &= \rho(\phi^n) (u^{n+1} \cdot \nabla u^n + u^n \cdot \nabla u^{n+1}), \\ T_2^n &= u^n \cdot \nabla \phi^n \frac{\rho_2 - \rho_1}{2} u^{n+1} + u^{n+1} \cdot \nabla \phi^n \frac{\rho_2 - \rho_1}{2} u^n, \end{aligned}$$

$$\begin{aligned}
T_3^n &= -\lambda_0 b (\nabla \theta^n \cdot \nabla \phi^{n+1}) \nabla \phi^n - \lambda_0 b (\nabla \theta^n \cdot \nabla \phi^n) \nabla \phi^{n+1} + \lambda (\theta^n) \Delta \phi^{n+1} \nabla \phi^n \\
&\quad + \lambda (\theta^n) \Delta \phi^n \nabla \phi^{n+1} + \lambda_0 b (\nabla \phi^n \cdot \nabla \phi^{n+1}) \nabla \theta^n - \lambda_0 b (\nabla \theta^{n+1} \cdot \nabla \phi^n) \nabla \phi^n \\
&\quad - \nabla \cdot \left( \frac{2\lambda (\theta^n)}{\varepsilon^2} ((\phi^n)^2 - 1) \phi^n \phi^{n+1} \right) - \lambda_0 b \theta^{n+1} \Delta \phi^n \nabla \phi^n \\
&\quad + \frac{\lambda_0 b}{2} \nabla \theta^{n+1} |\nabla \phi^n|^2 + \nabla \cdot \left( \frac{\lambda_0 b}{2\varepsilon^2} \theta^{n+1} ((\phi^n)^2 - 1)^2 \right), \\
T_4^n &= \frac{\rho_2 - \rho_1}{2} (u^n \cdot \nabla u^n \phi^{n+1} + u^n u^n \cdot \nabla \phi^{n+1}), \\
T_5^n &= \frac{\rho_2 - \rho_1}{2} (\beta - \alpha (\theta^n - \theta_0^n)) \phi^{n+1} \varphi g j, \\
S_1^n &= \rho (\phi^n) u^n \cdot \nabla u^n + 2u^n \cdot \nabla \phi^n \frac{\rho_2 - \rho_1}{2} u^n, \\
S_2^n &= -2\lambda_0 b (\nabla \theta^n \cdot \nabla \phi^n) \nabla \phi^n + \lambda_0 (a - 2b\theta^n) \Delta \phi^n \nabla \phi^n + \lambda_0 b \nabla \theta^n |\nabla \phi^n|^2 \\
&\quad + \nabla \cdot \left( \frac{2\lambda (\theta^n)}{\varepsilon^2} (\phi^n)^2 (1 - (\phi^n)^2) + \frac{\lambda_0 a}{2\varepsilon^2} ((\phi^n)^2 - 1)^2 \right), \\
S_3^n &= -\rho (\phi^n) (\alpha \theta_0^n + \beta) g \varphi j + \frac{\rho_2 - \rho_1}{2} (\beta - \alpha (\theta^n - \theta_0^n)) \varphi \phi^n g j, \\
S_4^n &= \frac{\rho_2 - \rho_1}{2} u^n \cdot \nabla u^n \phi^n, \quad n = 0, 1, 2, \dots
\end{aligned}$$

Similarly, the Newton's linearizations of phase field equation (2.17c) and energy equation (2.17d) are derived as follows

$$\begin{aligned}
&\phi_t^{n+1} + u^{n+1} \cdot \nabla \phi^n + u^n \cdot \nabla \phi^{n+1} - \gamma \Delta \phi^{n+1} + \frac{\gamma}{\varepsilon^2} (3(\phi^n)^2 - 1) \phi^{n+1} \\
&= u^n \cdot \nabla \phi^n + \frac{2\gamma}{\varepsilon^2} (\phi^n)^3, \tag{3.7}
\end{aligned}$$

and

$$\begin{aligned}
&\theta_t^{n+1} + u^n \cdot \nabla \theta^{n+1} + u^{n+1} \cdot \nabla \theta^n - k(\phi^n) \Delta \theta^{n+1} + \frac{k_1 - k_2}{2} \phi^{n+1} \Delta \theta^n \\
&= u^n \cdot \nabla \theta^n + \frac{k_1 - k_2}{2} \phi^n \Delta \theta^n. \tag{3.8}
\end{aligned}$$

Thus, we attain all of Newton's linearized equations for (2.17). In next section we will introduce the mixed finite element method for spatial discretization of (2.17) on the basis of these Newton's linearizations.

### 3.2 Mixed finite element method and nonlinear iterative algorithm

In order to design the mixed finite element discretizations for Newton's linearizations of (2.17), first of all, we derive the weak forms of linearized system of PDEs (3.6), (2.17b),

(3.7) and (3.8). Noticing that  $\Delta\phi^n$  exists in the coefficients of (3.6), so  $\phi \in H^2(\Omega)$ , specifically. We seek the weak solutions of the resulting variational forms in the following continuous spaces

$$V = [H^1(\Omega)]^d \times L^2(\Omega) \times H^2(\Omega) \times H^1(\Omega),$$

$$V_0 = [H_0^1(\Omega)]^d \times L^2(\Omega) \times (H^2(\Omega) \cap H_0^1(\Omega)) \times H_0^1(\Omega),$$

where  $u \in [H^1(\Omega)]^d, p \in L^2(\Omega), \phi \in H^2(\Omega), \theta \in H^1(\Omega)$  and are all subject to corresponding boundary conditions (2.18). Thus, the weak forms of (3.6), (2.17b), (3.7) and (3.8) can be defined as follows: given  $(u^n, p^n, \phi^n, \theta^n) \in V \times [0, T]$ , find  $(u^{n+1}, p^{n+1}, \phi^{n+1}, \theta^{n+1}) \in V \times [0, T]$ , such that for any  $(v, q, \xi, \zeta) \in V_0$ ,

$$\begin{aligned} & \left\langle \rho(\phi^n)u_t^{n+1} + \frac{\rho_2 - \rho_1}{2}\phi_t^n u^{n+1} - \rho(\phi^n)\phi\alpha g\theta^{n+1}j + \frac{\rho_2 - \rho_1}{2}(u_t^n\phi^{n+1} + u^n\phi_t^{n+1}) \right. \\ & \quad \left. + T_1^n + T_2^n + T_3^n + T_4^n + T_5^n, v \right\rangle + \langle \nu(\phi^n)\nabla u^{n+1}, \nabla v \rangle \\ & \quad + \left\langle \frac{\nu_2^n - \nu_1^n}{2}\phi^{n+1}\nabla u^n, \nabla v \right\rangle - \langle p^{n+1}, \nabla \cdot v \rangle + \langle \nabla \cdot u^{n+1}, q \rangle \\ & = \left\langle \frac{\rho_2 - \rho_1}{2}(u_t^n\phi^n + u^n\phi_t^n) + S_1^n + S_2^n + S_3^n + S_4^n, v \right\rangle + \left\langle \frac{\nu_2^n - \nu_1^n}{2}\phi^n\nabla u^n, \nabla v \right\rangle, \end{aligned} \tag{3.9}$$

$$\begin{aligned} & \langle \phi_t^{n+1} + u^{n+1} \cdot \nabla \phi^n + u^n \cdot \nabla \phi^{n+1}, \xi \rangle + \langle \gamma \nabla \phi^{n+1}, \nabla \xi \rangle \\ & \quad + \left\langle \frac{\gamma}{\varepsilon^2}(3(\phi^n)^2 - 1)\phi^{n+1}, \xi \right\rangle = \left\langle u^n \cdot \nabla \phi^n + \frac{2\gamma}{\varepsilon^2}(\phi^n)^3, \xi \right\rangle, \end{aligned} \tag{3.10}$$

and

$$\begin{aligned} & \langle \theta_t^{n+1} + u^n \cdot \nabla \theta^{n+1} + u^{n+1} \cdot \nabla \theta^n, \zeta \rangle + \langle k(\phi^n)\nabla \theta^{n+1}, \nabla \zeta \rangle \\ & \quad + \left\langle \frac{k_1 - k_2}{2}\phi^{n+1}\Delta \theta^n, \zeta \right\rangle = \left\langle u^n \cdot \nabla \theta^n + \frac{k_1 - k_2}{2}\phi^n\Delta \theta^n, \zeta \right\rangle, \end{aligned} \tag{3.11}$$

where  $n = 0, 1, 2, \dots$ ,  $\langle \cdot, \cdot \rangle$  denotes  $L^2$  inner product defined as  $\langle p, q \rangle = \int_{\Omega} pq dx$ . By Lax-Milgram and Babuška-Brezzi theorems ([32] and its references), it is well known that above weak forms exist unique weak solutions  $(u^{n+1}, p^{n+1}, \phi^{n+1}, \theta^{n+1}) \in V \times [0, T]$  in terms of the assumptions of sufficient smoothness, continuousness and coerciveness of coefficient functions in (2.17).

To obtain the numerical discretizations of (3.9)-(3.11), we adopt a type of stable mixed finite element, Taylor-Hood element ( $P_2P_1$  for triangle element or  $Q_2Q_1$  for rectangle element), to quadratically approximate velocity  $u$  and linearly approximate pressure  $p$  simultaneously in the saddle-point variational problem (3.9), and employ standard finite element method to discretize the equations of both phase field and thermal energy. where we use quadratic element to approximate phase field solution  $\phi$  since  $\phi \in H^2(\Omega)$ .

We define a quasi-uniform triangulation  $\mathcal{T}_h$  in a polygon domain  $\Omega$  with mesh size  $h$ , and introduce finite element space  $V_h = (P^2)^d \times P^1 \times P^2 \times P^1$  into  $\mathcal{T}_h$ , where  $P^2$  and  $P^1$  denote the piecewise quadratic and piecewise linear polynomial space, respectively. Meanwhile, we consider a uniform partition for time scale  $[0, T]$  with time step size  $\Delta t$  and

define  $t_k = k\Delta t$  ( $k=0,1,\dots,N$ ), where  $N = T/\Delta t$ . In the following we derive a full discrete mixed finite element approximations for spatial discretization of (3.9)-(3.11), combining with backward Euler scheme for temporal discretization.

Suppose solutions

$$(u_k, p_k, \phi_k, \theta_k) = (u(t_k), p(t_k), \phi(t_k), \theta(t_k))$$

at the  $k$ th time step have been attained for  $k=0,1,\dots,N-1$  (if  $k=0$ , then we take initial conditions

$$(u_0, p_0, \phi_0, \theta_0) = (u_0(x), p_0(x), \phi_0(x), \theta_0(x))).$$

To find solutions  $(u_{k+1}, p_{k+1}, \phi_{k+1}, \theta_{k+1})$  at the  $(k+1)$ th time step, we solve the Newton's linearized system of variational equations (3.9)-(3.11) iteratively by treating  $(u_k, p_k, \phi_k, \theta_k)$  as the initial guesses of nonlinear iteration at the  $(k+1)$ th time step, i.e.,

$$(u_{k+1}^0, p_{k+1}^0, \phi_{k+1}^0, \theta_{k+1}^0) = (u_k, p_k, \phi_k, \theta_k).$$

In the end,

$$(u_{k+1}, p_{k+1}, \phi_{k+1}, \theta_{k+1}) = \lim_{n \rightarrow \infty} (u_{k+1}^{n+1}, p_{k+1}^{n+1}, \phi_{k+1}^{n+1}, \theta_{k+1}^{n+1}).$$

Thus, the full discrete numerical schemes of (3.9)-(3.11) can be presented as follows: find  $(u_{k+1}^{n+1}, p_{k+1}^{n+1}, \phi_{k+1}^{n+1}, \theta_{k+1}^{n+1}) \in V_h \times [0, T]$ , such that for any  $(v, q, \xi, \zeta) \in V_h \times [0, T]$ ,

$$\begin{aligned} & \frac{1}{\Delta t} \left\langle \rho(\phi_{k+1}^n) u_{k+1}^{n+1} + \frac{\rho_2 - \rho_1}{2} (\phi_{k+1}^n - \phi_k) u_{k+1}^{n+1} + \frac{\rho_2 - \rho_1}{2} (u_{k+1}^n - u_k) \phi_{k+1}^{n+1} \right. \\ & \quad \left. + \frac{\rho_2 - \rho_1}{2} u_{k+1}^n \phi_{k+1}^{n+1}, v \right\rangle + \langle T_{1,k+1}^n + T_{2,k+1}^n + T_{3,k+1}^n + T_{4,k+1}^n + T_{5,k+1}^n \\ & \quad - \rho(\phi_{k+1}^n) \varphi \alpha g \theta_{k+1}^{n+1} j, v \rangle + \langle \nu(\phi_{k+1}^n) \nabla u_{k+1}^{n+1}, \nabla v \rangle \\ & \quad + \left\langle \frac{v_2^n - v_1^n}{2} \phi_{k+1}^{n+1} \nabla u_{k+1}^n, \nabla v \right\rangle - \langle p_{k+1}^{n+1}, \nabla \cdot v \rangle + \langle \nabla \cdot u_{k+1}^{n+1}, q \rangle \\ = & \frac{1}{\Delta t} \left\langle \rho(\phi_{k+1}^n) u_k + \frac{\rho_2 - \rho_1}{2} (\phi_{k+1}^n - \phi_k) u_{k+1}^n + \frac{\rho_2 - \rho_1}{2} (u_{k+1}^n - u_k) \phi_{k+1}^n \right. \\ & \quad \left. + \frac{\rho_2 - \rho_1}{2} u_{k+1}^n \phi_k, v \right\rangle + \langle S_{1,k+1}^n + S_{2,k+1}^n + S_{3,k+1}^n + S_{4,k+1}^n, v \rangle \\ & \quad + \left\langle \frac{v_2^n - v_1^n}{2} \phi_{k+1}^n \nabla u_{k+1}^n, \nabla v \right\rangle, \end{aligned} \tag{3.12}$$

$$\begin{aligned} & \left\langle \frac{1}{\Delta t} \phi_{k+1}^{n+1}, \xi \right\rangle + \langle \gamma \nabla \phi_{k+1}^{n+1}, \nabla \xi \rangle \\ & \quad + \langle u_{k+1}^{n+1} \cdot \nabla \phi_{k+1}^n + u_{k+1}^n \cdot \nabla \phi_{k+1}^{n+1}, \xi \rangle + \left\langle \frac{\gamma}{\varepsilon^2} (3(\phi_{k+1}^n)^2 - 1) \phi_{k+1}^{n+1}, \xi \right\rangle \\ = & \left\langle \frac{1}{\Delta t} \phi_k + u_{k+1}^n \cdot \nabla \phi_{k+1}^n + \frac{2\gamma}{\varepsilon^2} (\phi_{k+1}^n)^3, \xi \right\rangle, \end{aligned} \tag{3.13}$$

and

$$\begin{aligned}
 & \left\langle \frac{1}{\Delta t} \theta_{k+1}^{n+1}, \zeta \right\rangle + \langle k(\phi_{k+1}^n) \nabla \theta_{k+1}^{n+1}, \nabla \zeta \rangle \\
 & + \langle u_{k+1}^n \cdot \nabla \theta_{k+1}^{n+1} + u_{k+1}^{n+1} \cdot \nabla \theta_{k+1}^n, \zeta \rangle + \left\langle \frac{k_2 - k_1}{2} \phi_{k+1}^{n+1} \nabla \theta_{k+1}^n, \nabla \zeta \right\rangle \\
 = & \left\langle \frac{1}{\Delta t} \theta_k + u_{k+1}^n \cdot \nabla \theta_{k+1}^n, \zeta \right\rangle + \left\langle \frac{k_2 - k_1}{2} \phi_{k+1}^n \nabla \theta_{k+1}^n, \nabla \zeta \right\rangle, \tag{3.14}
 \end{aligned}$$

where  $n = 0, 1, 2, \dots, k = 0, 1, \dots, N-1$ . There are two types of iteration processes are involved in (3.12)-(3.14): inner nonlinear iteration process denoted by the superscript  $n$  and outer time marching process denoted by the subscript  $k$ , which are described by Algorithm 3.1.

Algorithm 3.1:

- 
1. Initialization: set time step  $k=0$  and take initial conditions

$$(u_0, p_0, \phi_0, \theta_0) = (u_0(x), p_0(x), \phi_0(x), \theta_0(x)).$$

2. Outer time marching: march to the  $(k+1)$ th time step, and let  $t = (k+1)\Delta t$ . If  $t > T$ , then the entire computation ends.
3. Inner nonlinear iteration: set the iteration step No.  $n=0$  and take initial guesses

$$(u_{k+1}^0, p_{k+1}^0, \phi_{k+1}^0, \theta_{k+1}^0) = (u_k, p_k, \phi_k, \theta_k).$$

4. Finite element computation: iterate to the  $(n+1)$ th step, and solve (3.12)-(3.14) for their numerical solutions  $(u_{k+1}^{n+1}, p_{k+1}^{n+1}, \phi_{k+1}^{n+1}, \theta_{k+1}^{n+1})$ .
5. Investigation of stopping criteria for inner nonlinear iteration: if

$$(\|u_{k+1}^{n+1} - u_{k+1}^n\|_0^2 + \|p_{k+1}^{n+1} - p_{k+1}^n\|_0^2 + \|\phi_{k+1}^{n+1} - \phi_{k+1}^n\|_0^2 + \|\theta_{k+1}^{n+1} - \theta_{k+1}^n\|_0^2)^{\frac{1}{2}} \leq \text{tolerance},$$

then switch to step 2 and go to the next time step. Otherwise, back to step 4 and continue current nonlinear iteration.

---

Apparently (3.12)-(3.14) are full implicit schemes, it derives a nonsymmetric positive defined algebraic linear system at each time step. Since there are four degrees of freedom at each grid point, the computational cost of solving this algebraic system is not cheap, depending on the number of grid points and spatial dimension. We usually employ a preconditioned GMRES iterative solver to solve the derived large-scale algebraic system, which would result in the computation being  $\mathcal{O}(N \log(N))$ , a significant improvement for a large system. In our computation we adopt incomplete LU (ILU) preconditioner for GMRES solver with fill level 5 above.

Because phase field model turns out to be identical to a sharp-interface level-set formulation asymptotically [25] when the thickness of the interface approaches zero, i.e.

$\varepsilon = \mathcal{O}(h) \rightarrow 0$  as  $h \rightarrow 0$ , a local finer mesh around the interface, namely let  $h \rightarrow 0$  locally near interface, is a right approach to achieve higher accuracy for phase-field method. But meanwhile, due to the sharper interface of phase solution  $\phi$ , the numerical difficulties are also introduced to the entire computation such as instable nonlinear iteration. More techniques may be needed to conquer these problems, as we indicated in Section 4.

For the sake of precisely tracking the motion of the interface between fluid mixtures, a smaller mesh size  $h$  can be properly given around the interface area than elsewhere in our quasi-uniform triangulation  $\mathcal{T}_h$ , resulting in a relative expensive computation. It is still doable if we utilize an efficient and robust nonsymmetric iterative solver, such as ILU-preconditioned GMRES or BiCG-Stab, to solve the resulting large scale algebraic system, as we do in Section 4.

### 4 Numerical experiments

In this section we employ a concrete problem of two-phase flows associated with thermo-induced Marangoni effects to show the strengths of phase field method and the corresponding numerical algorithms demonstrated in Section 3.

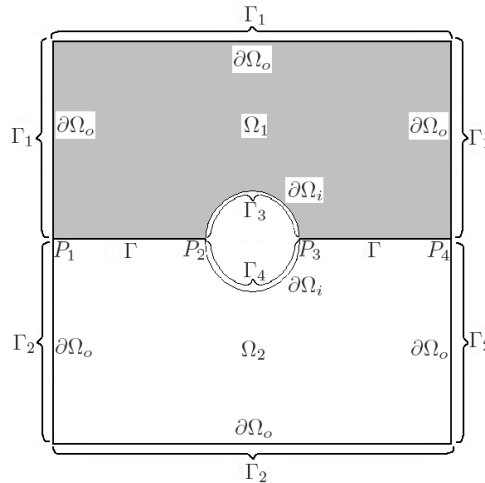


Figure 1: Domain  $\Omega$ .

To essentially illustrate the correctness and efficiency of our phase field model (2.17) and its numerical discretizations (3.12)-(3.14), we define (2.17) on a square domain  $\Omega = [0,2] \times [0,2] \cap \{(x,y) | (x-1)^2 + (y-1)^2 \geq 0.25\}$ , as shown in Fig. 1, and specifically equip it with two different temperature boundary conditions: one is heating inside (on the circle) and cooling outside (on the square boundary); and the other one is heating outside and cooling inside, conversely. Provided the fluid mixtures are contained in domain  $\Omega$ , these two cases of temperature boundary conditions will result in two different phenomena associated with thermo-induced Marangoni effects in the mixtures. In this way the do-

main  $\Omega$  can show a significant part of the solution: due to the thermo-induced surface tension heterogeneity on the interface, the interfacial motion between two-phase flows will present sine/cosine-like curve, depending on the direction of temperature gradient. In the following we will illustrate this dramatic thermo-induced Marangoni effect in domain  $\Omega$  by numerically simulating (3.12)-(3.14) with different temperature boundary conditions.

Let  $\partial\Omega_o$  and  $\partial\Omega_i$  denote the outer boundary and inner boundary of  $\Omega$ , respectively, then  $\partial\Omega = \partial\Omega_o \cup \partial\Omega_i$ . As shown in Fig. 1,  $\partial\Omega_o = \Gamma_1 \cup \Gamma_2$ ,  $\partial\Omega_i = \Gamma_3 \cup \Gamma_4$ . Let  $P_1, P_2, P_3$  and  $P_4$  represent four intersection points between boundary  $\partial\Omega$  and the horizontal midline  $\Gamma$ , where  $\Gamma$  is also adopted as the initial interface between two-phase flows.

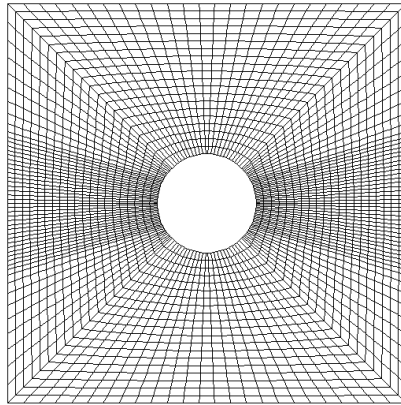


Figure 2: Triangulation  $\mathcal{T}_h$ .

We make a quasi-uniform triangulation  $\mathcal{T}_h$  in domain  $\Omega$  (see Fig. 2) in which the mesh size around the initial interface  $\Gamma$  is smaller than elsewhere. For simplicity's sake, we let two-phase flows hold the same physical parameters, e.g.  $\nu_1 = \nu_2 = 10, \rho_1 = \rho_2 = 1, k_1 = k_2 = 5$ , and assign other monitoring parameters arising in (2.17) to be  $\lambda_0 = 1, \gamma = 0.025, \varepsilon = 0.5h, a = 5, b = 1, \alpha = 10, g = 9.8$ . The combination of small mesh size  $h$  around interfacial area and small parameter  $c = 0.5$  associated with  $\varepsilon$  is able to attain a relatively small interface length  $\varepsilon = ch$ , which basically ensures a reliable numerical solution of phase  $\phi$  for phase field model (2.17).

By the theory of phase field method, although the phase field equation (2.17c) eventually approaches to the original transport equation as  $\gamma \rightarrow 0$ , and the interface length approximates the real case as  $\varepsilon \rightarrow 0$ , it is always crucial to choose these two parameters properly. Too small  $c$ , and further, too small  $\varepsilon$ , may introduce sharper interface into phase  $\phi$ , and too small  $\gamma$  may produce dominant convection problem. Both of these cases can make the nonlinear iteration instable and hard to converge. To achieve the balance between accuracy and efficiency, we reduce the time step size  $\Delta t$  in order to stabilize the entire computation. Numerical experiments also show us the smaller  $\Delta t$ , the stabler entire nonlinear iteration. In the following experiments, we take a small uniform time step size  $\Delta t = 0.0025$  in a time scale  $[0, 1]$ .

We introduce two cases of boundary conditions and initial conditions for (2.17) in domain  $\Omega$ . Except temperature  $\theta$ , in both cases velocity  $u$ , pressure  $p$  and phase field  $\phi$  hold the same boundary conditions and initial conditions, defined as follows.

### Common boundary conditions for velocity and phase

$$\begin{aligned} u|_{\partial\Omega} &= 0, & \phi|_{\Gamma_1 \setminus (P_1 \cup P_4) \cup \Gamma_3 \setminus (P_2 \cup P_3)} &= 1, \\ \phi|_{\Gamma_2 \setminus (P_1 \cup P_4) \cup \Gamma_4 \setminus (P_2 \cup P_3)} &= -1, & \phi|_{P_1 \cup P_2 \cup P_3 \cup P_4} &= 0, \end{aligned} \quad (4.1)$$

where we specifically assign Dirichlet boundary condition for  $\phi$ , which implies that the intersection points of phase interface and boundary  $\partial\Omega$ , on which  $\phi = 0$ , is fixed.

### Common initial conditions for velocity and phase

$$\begin{aligned} u_0(x) &= p_0(x) = 0 \quad (x \in \Omega), \\ \phi_0(x) &= 1 \quad (x \in \Omega_1), \quad \phi_0(x) = -1 \quad (x \in \Omega_2), \quad \phi_0(x) = 0 \quad (x \in \Gamma). \end{aligned} \quad (4.2)$$

Such initial condition for  $\phi$  gives the initial position of phase interface as horizontal mid-line  $\Gamma$ .

### Specific boundary and initial conditions for temperature

We investigate two cases here by switching heating and cooling places on  $\partial\Omega_o$  and  $\partial\Omega_i$ , respectively:

*Case 1: Heating inside and cooling outside.*

$$\theta|_{\partial\Omega_i} = 10, \quad \theta|_{\partial\Omega_o} = 0; \quad \theta_0(x)|_{\partial\Omega_i} = 10 \quad \text{and} \quad \theta_0(x) = 0 \quad \text{elsewhere.} \quad (4.3)$$

*Case 2: Heating outside and cooling inside.*

$$\theta|_{\partial\Omega_i} = 0, \quad \theta|_{\partial\Omega_o} = 10; \quad \theta_0(x)|_{\partial\Omega_o} = 10 \quad \text{and} \quad \theta_0(x) = 0 \quad \text{elsewhere.} \quad (4.4)$$

In the following we will numerically study the above two cases and illustrate their numerical solutions in details, respectively.

#### 4.1 Case 1: Heating inside and cooling outside

By solving (3.12)-(3.14) along with boundary conditions and initial conditions (4.1), (4.2) and (4.3) in terms of Algorithm 3.1, we obtain a series of numerical results as illustrated by Figs. 3-6.

Given the case of heating inside and cooling outside, and beginning with an initial horizontal midline  $\Gamma$ , Fig. 3 shows that the phase interface eventually evolves to a sine/cosine-like curve due to thermo-induced surface tension. When time marches longer, this curve turns out to be steeper.

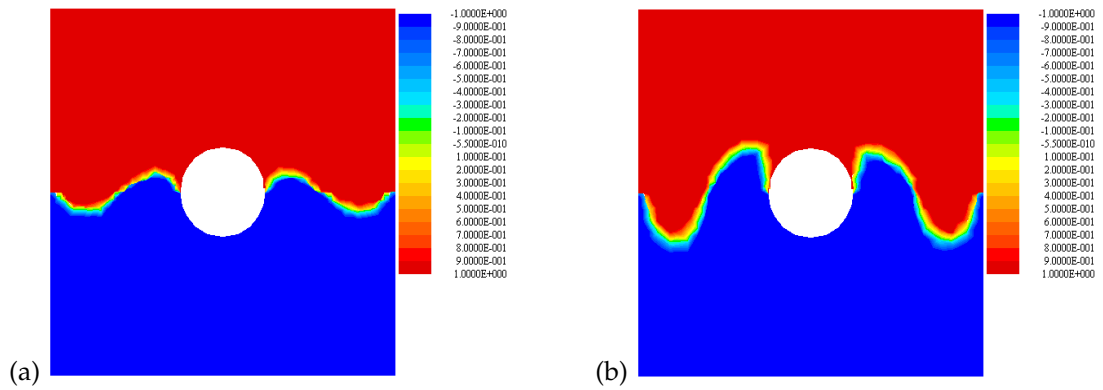


Figure 3: Phase field for Case 1 at (a)  $t=0.25$ , and (b)  $t=1$ .

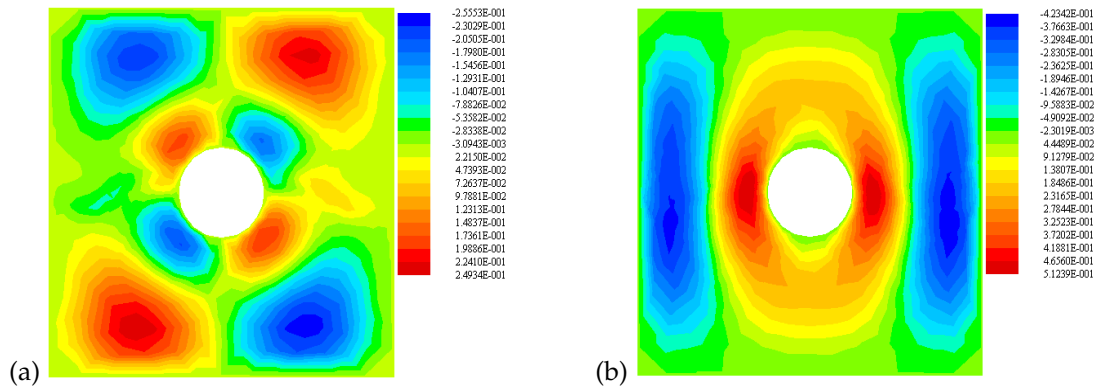


Figure 4: Horizontal velocity (a) and vertical velocity (b) for Case 1 at  $t=1$ .

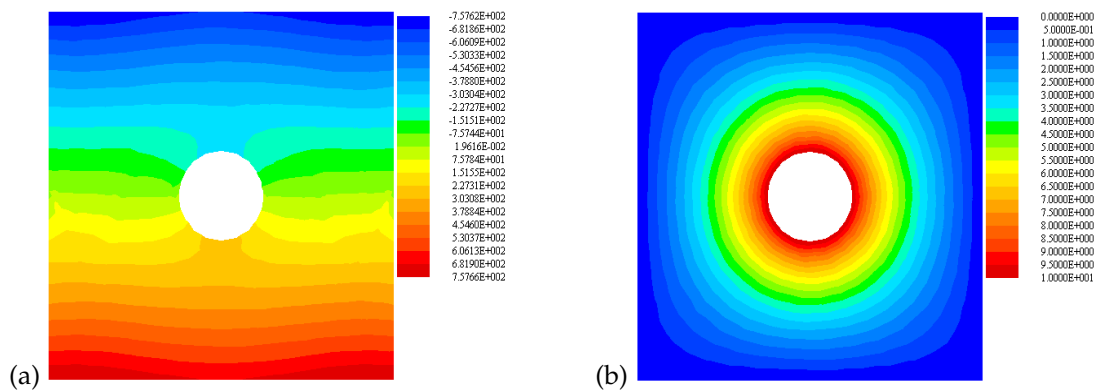


Figure 5: Pressure (a) and temperature (b) for Case 1 at  $t=1$ .

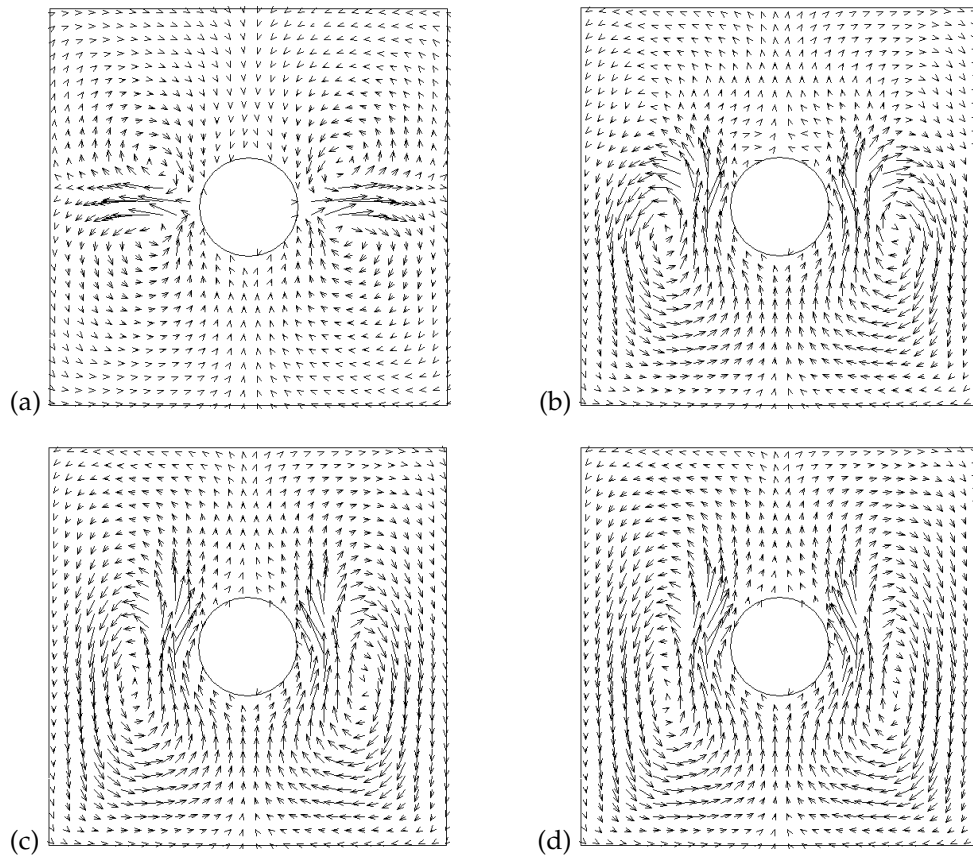


Figure 6: Velocity field for Case 1 at (a)  $t=0.0025$ , (b)  $t=0.03$ , (c)  $t=0.06$  and (d)  $t=0.09$ .

Under the boundary conditions of *Case 1*, the resulting numerical solutions illustrate that the thermal energy plays a fundamental role in the interfacial dynamics of two-phase flows. In particular, it gives rise to a dynamic interfacial tension that depends on the direction of temperature gradient, determining the movement of the interface along a sine/cosine-like curve.

#### 4.2 Case 2: Heating outside and cooling inside

Conversely, if switching the places of heating and cooling in *Case 1*, namely substituting temperature's boundary and initial conditions (4.4) for (4.3), then we attain another series of numerical results which are the converse solutions of *Case 1*, as displayed by Figs. 7-10, where the interface presents flip vertical of that of *Case 1* because of the converse of temperature boundary condition, and further, the converse of the direction of temperature gradient, which eventually reverse the direction of interfacial tension.

As far as we know, there has been no report of experimental observation of such thermo-induced Marangoni flows. This is the first time we investigate this interesting

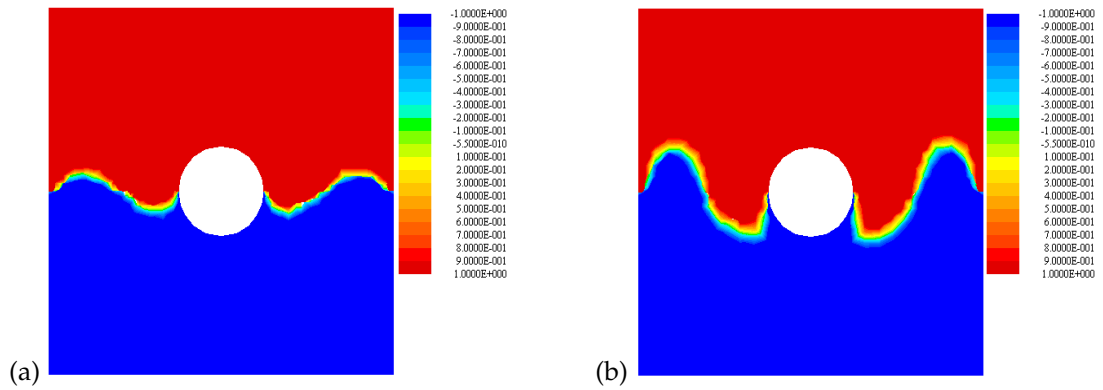


Figure 7: Phase field for Case 2 at (a)  $t=0.25$ , and (b)  $t=1$ .

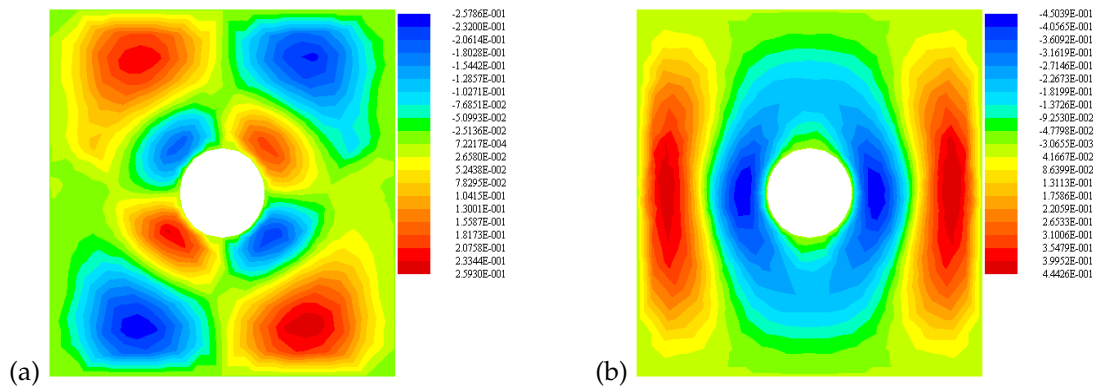


Figure 8: Horizontal velocity (a) and vertical velocity (b) for Case 2 at  $t=1$ .

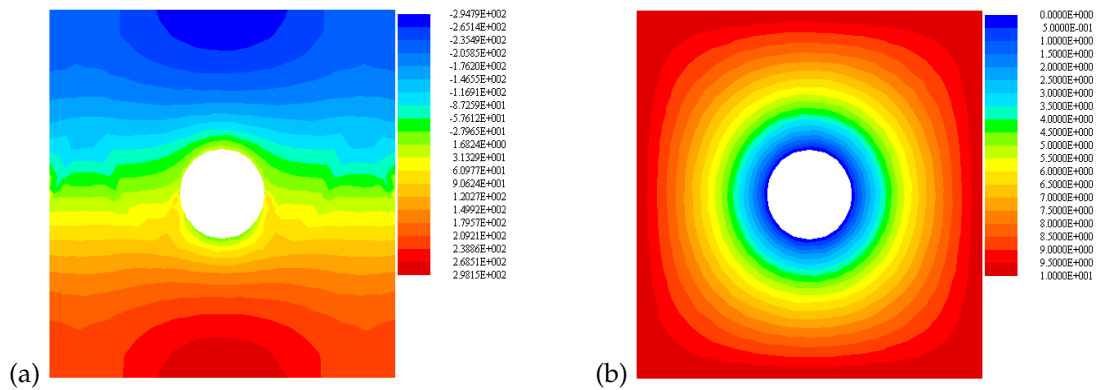


Figure 9: Pressure (a) and temperature (b) for Case 2 at  $t=1$ .

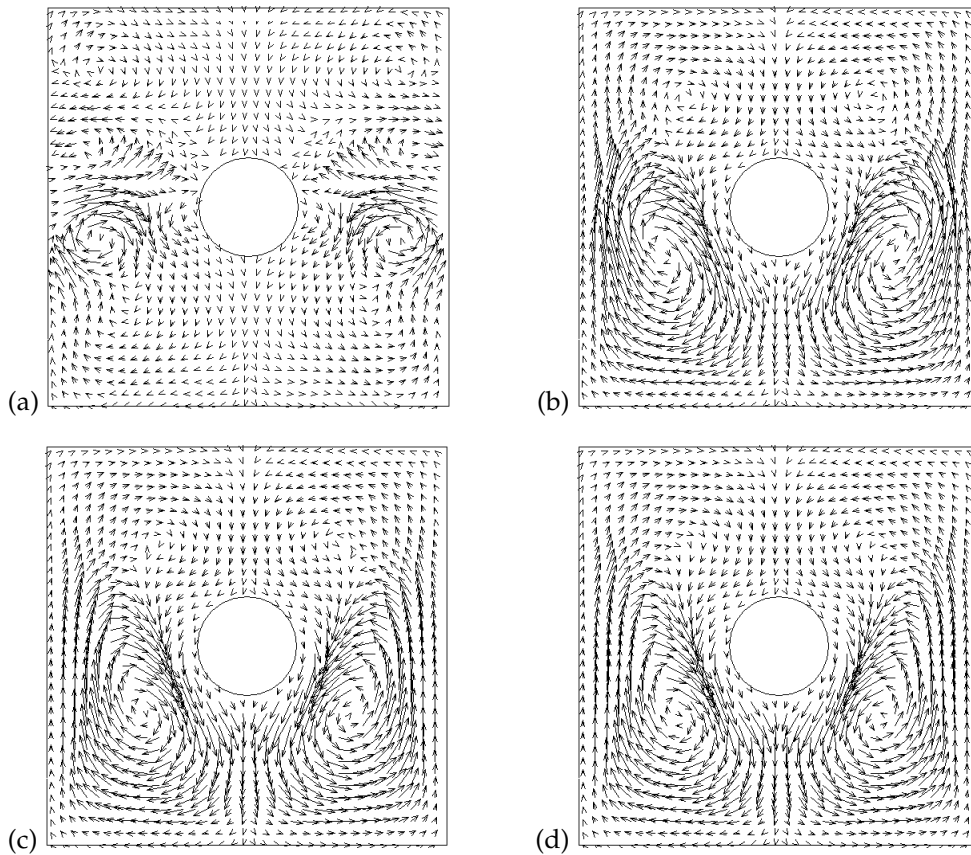


Figure 10: Velocity field for Case 2 at (a)  $t=0.0025$ , (b)  $t=0.03$ , (c)  $t=0.06$  and (d)  $t=0.09$ .

two-phase flows mainly driven by thermal transformation in numerical approaches. The dramatic changes occurring to the movement of interfaces physically make sense, and consequently, it justifies that our mathematical model derived from the phase field theory basically reflects the mechanism of thermo-induced Marangoni effects in the fluid mixtures.

## 5 Conclusions

A phase field model (2.17) about thermo-induced Marangoni effects in the mixtures is studied in this paper, a strongly nonlinear system of PDE is derived which combines Navier-Stokes equations with phase field and energy transport equations. An additional term with respect to phase and temperature is added into momentum equation to simulate temperature-induced surface tension effect. An fully implicit mixed finite element method along with total Newton's linearization is developed specifically for this phase field model to numerically investigate the motion of interface involving in the thermo-

induced two-phase flows. Two typical numerical experiments are carried out with presented numerical methods. Numerical solutions illustrate dramatic thermal induced Marangoni effects in the mixtures, the interfacial motion and corresponding surface tension's change are influenced greatly by the direction of temperature gradient, which demonstrates that thermo-induced surface tension plays an important role to drive interfaces among fluid mixtures. As a result, it also indicates that phase field model (2.17) is a right mathematical representation to reflect thermo-induced Marangoni effects in the mixtures.

By phase field theory, to precisely solve Marangoni effect in the fluid mixtures, the interface length  $\epsilon$ , which is proportional to mesh size  $h$ , has to approximate 0 as possible as we can. In numerical implementation, this is nontrivial work since the sharper interface will be introduced to the solution. Thus, an efficient adaptive local refined mesh [34] would be helpful to catch up and resolve the moving sharp interface. Such work is under way to incorporate the phase field theory and simulate above two-phase flow problems with adaptive finite element method.

## Acknowledgments

Pengtao Sun was supported in part by Research Development Award of University of Nevada Las Vegas 2220-320-980C. Chun Liu was supported in part by National Science Foundation Grant DMS-0707594. Jinchao Xu was supported in part by National Science Foundation Grant DMS-0609727 and Alexander H. Humboldt Foundation. This work was also supported by the Center for Computational Mathematics and Applications of Penn State.

## References

- [1] N. D. Alikakos, P. W. Bates, and X. F. Chen, Convergence of the Cahn-Hilliard equation to the Hele-Shaw model, *Arch. Rational Mech. Anal.*, 128 (1994), pp. 165-205.
- [2] D. M. Anderson and G. B. McFadden, A diffuse-interface description of internal waves in a near-critical fluid, *Phys. Fluids*, 9 (1997), pp. 1870-1879.
- [3] D. M. Anderson, G. B. McFadden and A. A. Wheeler, Diffuse-interface methods in fluid mechanics, *Appl. Math. Lett.*, 30 (1998), pp. 139-165.
- [4] T. Blesgen, A generalization of the navier-stokes equations to two phase flow, Preprint, (2000).
- [5] F. Boyer, Mathematical study of multi-phase flow under shear through order parameter formulation, *Asymptot. Anal.*, 20 (1999), pp. 175-212.
- [6] F. Boyer, A theoretical and numerical model for the study of incompressible mixture flows, *Computers and Fluids*, 31 (2002), pp. 41-68.
- [7] L. Bronsard and R. Kohn, Motion by mean curvature as the singular limit of Ginzburgh-Landau model, *J. Diff. Eqns*, 90 (1991), pp. 211-237.
- [8] L. Bronsard and R. V. Kohn, On the slowness of phase boundary motion in one space dimension, *Comm. Pure Appl. Math.*, 43 (1990), pp. 983-997.

- [9] G. Caginalp and X. F. Chen, Phase field equations in the singular limit of sharp interface problems, in *On the evolution of phase boundaries* (Minneapolis, MN, 1990–91), Springer, New York, 1992, pp. 1-27.
- [10] J. W. Cahn and S. M. Allen, A microscopic theory for domain wall motion and its experimental verification in Fe-Al alloy domain growth kinetics, *J. Phys. Colloque*, 38 (1977), pp. C7-51.
- [11] J. W. Cahn and J. E. Hillard, Free energy of a nonuniform system. I. Interfacial free energy, *J. Chem. Phys.*, 28 (1958), pp. 258-267.
- [12] Y. C. Chang, T. Y. Hou, B. Merriman, and S. Osher, A level set formulation of eulerian interface capturing methods for incompressible fluid flows., *J. Comput. Phys.*, 124 (1996), pp. 449-464.
- [13] H. Chen, D. Jasnow, and J. Viñals, Interface and contact line motion in a two phase fluid under shear flow, *Phys. Rev. Lett.*, 85 (1986), pp. 1686-1689.
- [14] D. L. Denny and R. L. Pego, Models of low-speed flow for near-critical fluids with gravitational and capillary effects, *Quart. Appl. Math.*, 58 (2000), pp. 103-125.
- [15] J. E. Dunn and J. Serrin, On the thermomechanics of interstitial working, *Arch. Rational Mech. Anal.*, 88 (1985), pp. 95-133.
- [16] W. E and P. Palffy-Muhoray, Phase separation in incompressible systems, *Phys. Rev. E* (3), 55 (1997), pp. R3844-R3846.
- [17] L. C. Evans, H. M. Soner, and P. E. Souganidis, Phase transitions and generalized motion by mean curvature, *Comm. Pure Appl. Math.*, 45 (1992), pp. 1097-1123.
- [18] M. E. Gurtin, D. Polignone, and J. Viñals, Two-phase binary fluids and immiscible fluids described by an order parameter, *Math. Models Methods Appl. Sci.*, 6 (1996), pp. 815-831.
- [19] D. Jacqmin, Calculation of two-phase Navier-Stokes flows using phase-field modeling, *J. Comput. Phys.*, 155 (1999), pp. 96-127.
- [20] D. D. Joseph, Fluid dynamics of two miscible liquids with diffusion and gradient stresses, *European J. Mech. B Fluids*, 9 (1990), pp. 565-596.
- [21] R. G. Larson, *The Structure and Rheology of Complex Fluids*, Oxford, 1995.
- [22] C. Liu and J. Shen, A phase field model for the mixture of two incompressible fluids and its approximation by a fourier-spectral method, *Physica D*, 179 (2002), pp. 211-228.
- [23] C. Liu and S. Shkoller, Variational phase field model for the mixture of two fluids, preprint, (2001).
- [24] C. Liu and N. J. Walkington, An eulerian description of fluids containing visco-hyperelastic particles, *Arch. Rat. Mech. Ana.*, 159 (2001), pp. 229-252.
- [25] J. Lowengrub and L. Truskinovsky, Quasi-incompressible Cahn-Hilliard fluids and topological transitions, *R. Soc. Lond. Proc. Ser. A Math. Phys. Eng. Sci.*, 454 (1998), pp. 2617-2654.
- [26] G. B. McFadden, A. A. Wheeler, and D. M. Anderson, Thin interface asymptotics for an energy/entropy approach to phase-field models with unequal conductivities, *Phys. D*, 144 (2000).
- [27] G. B. McFadden, A. A. Wheeler, R. J. Braun, S. R. Coriell, and R. F. Sekerka, Phase-field models for anisotropic interfaces, *Phys. Rev. E* (3), 48 (1993), pp. 2016-2024.
- [28] W. W. Mullins and R. F. Sekerka, On the thermodynamics of crystalline solids, *J. Chem. Phys.*, 82 (1985).
- [29] T. Qian, X. P. Wang, and P. Sheng, Molecular scale contact line hydrodynamics of immiscible flows, preprint, (2002).
- [30] J. Rubinstein, P. Sternberg, and J. B. Keller, Fast reaction, slow diffusion, and curve shortening, *SIAM J. Appl. Math.*, 49 (1989), pp. 116-133.
- [31] J. E. Taylor and J. W. Cahn, Linking anisotropic sharp and diffuse surface motion laws via

- gradient flows, *J. Statist. Phys.*, 77 (1994), pp. 183-197.
- [32] A. Quarteroni and A. Valli, *Numerical Approximation of Partial Differential Equations*, Springer Series in Computational Mathematics, 23 (1997).
- [33] T. Zhang, N. Cogan and Q. Wang Phase-field models for biofilms II. 2-D numerical simulations of biofilm-flow interaction, *Commun. Comput. Phys.*, 4(2008), pp. 72-101.
- [34] P. Sun, R. D. Russell, and J. Xu, A new adaptive local mesh refinement algorithm and its application on fourth order thin film flow problem, *J. Comput. Phys.*, 224(2007), pp. 1021-1048.
- [35] P. Yue, J. Feng, C. Liu and J. Shen, Interfacial forces and Marangoni flow on a nematic drop retracting in an isotropic fluid, *Journal of Colloid and Interface Science*, 290(2005), pp. 281-288.
- [36] C. V. Sternling and E. Scriven, Interfacial Turbulence: Hydrodynamic instability and the marangoni effect, *A.I.Ch.E. Journal*, 5(1959), pp. 514-523.